Propofol Administration During Early Postnatal Life Suppresses Hippocampal Neurogenesis

8 authors, including:

Xi Chen
Nankai University
7 PUBLICATIONS 49 CITATIONS

SEE PROFILE

Xiaotang Fan
Third Military Medical University
61 PUBLICATIONS 942 CITATIONS

SEE PROFILE

Some of the authors of this publication are also working on these related projects:

Project Hippocampus neurogenesis View project

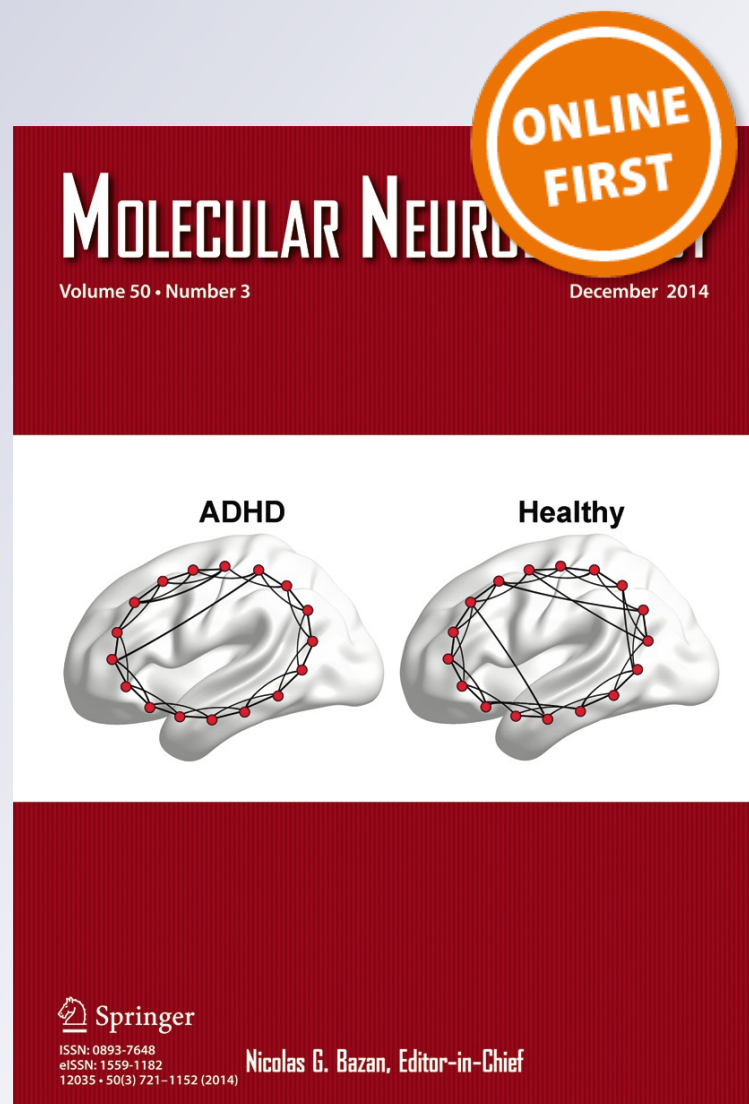# Propofol Administration During Early Postnatal Life Suppresses Hippocampal Neurogenesis

Jing Huang, Sheng Jing, Xi Chen, Xiaohang Bao, Zhiyong Du, Hong Li, Tiande Yang & Xiaotang Fan

Molecular Neurobiology
Volume 50 · Number 3
December 2014

ADHD   Healthy

Springer
ISSN: 0893-7648
eISSN: 1559-1182
12035 · 50(3) 721–1152 (2014)
Nicolas G. Bazan, Editor-in-Chief

Springer

Propofol Administration During Early Postnatal Life Suppresses Hippocampal Neurogenesis

Jing Huang · Sheng Jing · Xi Chen · Xiaohang Bao ·
Zhiyong Du · Hong Li · Tiande Yang · Xiaotang Fan

Abstract Propofol is currently one of the most widely used intravenous anesthetics and has been indicated to induce cognitive dysfunction in adults. Here, we investigated the effects of propofol exposure during early postnatal life on hippocampal neurogenesis. Propofol (30 or 60 mg/kg) was administered to mice on either postnatal day (P) 7 or P7–P9; cell proliferation and neurogenesis in the dentate gyrus (DG) were evaluated on P8 or P17. It showed that exposure to propofol on P7 decreased hippocampal cell proliferation as indicated by BrdU and Sox2 immunostaining at P8 in propofol treatment at the dosage of 60 mg/kg but not at the dosage of 30 mg/kg. Western blots revealed propofol treatment decreased Akt or extracellular signal-related kinase (ERK) 1/2 phosphorylation in the hippocampus at P8. Propofol treatment on P7 to P9 reduced the numbers of newly formed neurons in the DG at P17, which was accompanied by delay of granule neuron maturation and decreased the density of dendritic spines, particularly the mushroom-shaped mature spines. Furthermore, the in vitro findings indicated propofol suppressed cell proliferation and cell mitosis and activated apoptosis of C17.2 neural stem cell line in a dose-dependent manner. These findings suggest that propofol impairs cell proliferation and inhibits neurogenesis in the immature mouse brain and thus is possibly involved in the cognitive dysfunction induced by propofol anesthesia.

Keywords Propofol · Hippocampus · Neurogenesis · Neurotoxicity · Mouse

Introduction

General anesthesia is commonly used in pediatric surgery of neonates and young children [1–3]. However, the developing brain is more vulnerable to anesthetic-induced neurotoxicity, which can produce long-term neurocognitive deficits. Experimental studies have demonstrated that general anesthetics induce a profound neuroapoptosis in the developing brain, which thereby leads to neurobehavioral and functional deficits in animals [4–9]. A clinical study by Wilder and colleagues also found that multiple anesthesia exposure before age four could induce high incidences of learning disability in children [10]. Therefore, there needs to be concern with the safety of general anesthesia when used in pediatric medicine.

Propofol is a widely used general anesthetic that enhances the action of γ-amino butyric acid (GABA) through the GABA A (GABA$_A$) receptor and blocks the N-methyl-D-aspartate (NMDA) glutamate receptor [11–13]. Studies in rodents have demonstrated that both single dose and repeated doses of propofol exposure during brain development cause neuronal apoptosis and degeneration [4, 6, 8, 9, 14]. Moreover, anesthetic neurotoxicity depends on the period of vulnerability for exposure, and anesthetic-induced neuronal apoptosis appeared during the first 2 weeks after birth in rodents, peaking at postnatal day (P) 7 [7, 15, 16]. However, propofol-

Jing Huang and Sheng Jing contributed equally to this work.

J. Huang · S. Jing · X. Bao · Z. Du · H. Li · T. Yang (✉)
Department of Anesthesiology, Xinqiao Hospital, Third Military Medical University, Chongqing 400037, People's Republic of China
e-mail: 31011@sina.com

X. Chen
School of Medicine, Nankai University, Tianjin 300071, People's Republic of China

X. Chen
Department of Ophthalmology, Chinese People's Liberation Army General Hospital, Beijing 100853, People's Republic of China

X. Fan (✉)
Department of Developmental Neuropsychology, School of Psychology, Third Military Medical University, Chongqing 400038, People's Republic of China
e-mail: fanxiaotang2005@163.com

induced neurotoxic effects involve more than neuronal apoptosis and necrosis during the period of brain vulnerability.

It is well known that new neurons are produced in the postnatal hippocampus [17] and play a functional role in cognitive processes such as learning and memory [18–20]. Recent studies indicate that propofol modulates hippocampal neurogenesis [21–23]. It has been found that propofol impairs survival and maturation of adult-born hippocampal neurons in a developmental manner in mice [24]. In addition, propofol significantly decreased the number of differentiating neurons and increased the number of astrocytes in the dentate gyrus (DG) of 3-month-old rats [21]. On the contrary, an in vitro study has confirmed that clinical relevant doses of propofol increase neuronal fate choice of cultured neural precursor cells (NPCs) [25]. It appears that propofol exerts different effects that depend on the dosage and the developmental period of administration. However, the effect of propofol on hippocampal neurogenesis during the first 2 weeks after birth is still unexplored.

In this study, newborn mice at P7 were treated with single injection of 30 or 60 mg/kg of propofol or vehicle of equal volume to explore the effect of propofol on the proliferation of NPCs. They were also treated with repeated injections from P7 to P9 to determine the influences of propofol on early neurogenesis, including neuronal differentiation and maturation of newborn neurons and dendrite spines in the hippocampal DG. As the activation of extracellular signal-related kinase (ERK) and Akt pathway has been reported to play crucial roles in the regulation of self-renewing and differentiation of NPCs during the development of the hippocampus [26], their involvement in the underlying mechanism of propofol on the modulation of hippocampal neurogenesis during the early stage was also explored. Finally, the effect of propofol was tested in vitro using the multipotent neural stem cell (NSC) line C17.2 by analyzing the cell proliferation, apoptosis, and cell cycle with immunocytochemistry and flow cytometric analysis (FACS), respectively.

Materials and Methods

Animals

Male and female C57/BL6 mice were provided by the Third Military Medical University and housed in a temperature-controlled room with a standard 12-h light/12-h dark cycle and ad libitum access to food and water. All experimental procedures were approved by the Third Military Medical University and performed according to the guidelines for laboratory animal care and use. All efforts were made to reduce the number of animals used and their suffering. Except for the brief intervals of separation required for daily injection, the pups were kept with their dams throughout the experiment.

Throughout all experiments, control and experimental pups were drawn randomly from the same litters.

Drug Treatment

The day of birth was designated as P0. To assess the effect of propofol on the cell proliferation in the DG of mice, pups received vehicle or propofol intraperitoneally (i.p.) on P7 and were treated with BrdU (50 mg/kg) on P8 (Fig. 1a). Propofol was administered at a dose of 30 or 60 mg/kg. An equivalent volume of i.p. administered intralipid was used as a vehicle control for propofol. Pups were sacrificed 2 h after BrdU injection.

To study whether neurogenesis in the subgranular zone (SGZ) and the granular cell layer (GCL) of the DG on P17 would be affected by drug treatment, we chose the following treatment protocol: the animals received i.p. injections of propofol at a dose of 30 or 60 mg/kg, on three subsequent days beginning on P7 (Fig. 1b). An equivalent volume of i.p. administered intralipid was used as a vehicle control for propofol. BrdU was administered at a dose of 50 mg/kg on P10, and pups were sacrificed on P17. Their brains were processed for NeuN immunohistochemical staining and double immunohistochemical staining for BrdU and DCX.

In all experiments, all of the mice were initially anesthetized in their home cage, and, once sedated, they were transferred to a Thermocare® ICS therapy warmer unit (Thermocare, Incline Village, NV, USA) set to maintain a mouse body temperature of 37 °C [27].

Immunohistochemistry and Immunofluorescence

For perfusion fixation, mice were deeply anesthetized with an overdose of isoflurane and transcardially perfused with 0.01 M phosphate-buffered saline (PBS, pH 7.4) for 5 to 10 min followed by 4 % paraformaldehyde in 0.1 M phosphate buffer (PB, pH 7.4) for 15 to 20 min. The whole brains were removed and postfixed in the same fixative for 3 to 4 days at 4 °C. Animal body and brain weights were documented for each experiment.

Immunohistochemistry was performed with cryostat sections (40 μm at P8 or 20 μm at P17). The sections were incubated in 0.5 % H_2O_2 in PBS for 30 min at room temperature to quench endogenous peroxidase and then incubated in 0.5 % Triton X-100 in PBS for 30 min. To block nonspecific binding, the sections were incubated in 3 % bovine serum albumin (BSA) for 1 h at 4 °C. The sections were incubated with primary antibodies in 1 % BSA (12 h, 4 °C): rabbit polyclonal anti-sex-determining region Y (SRY)-box 2 (Sox2, 1:1000, Chemicon, USA) and mouse anti-NeuN (1:500, Millipore, USA). BSA replaced primary antibodies in the negative controls. For Sox2 staining, the sections were incubated with the biotinylated secondary antibody (1:200;
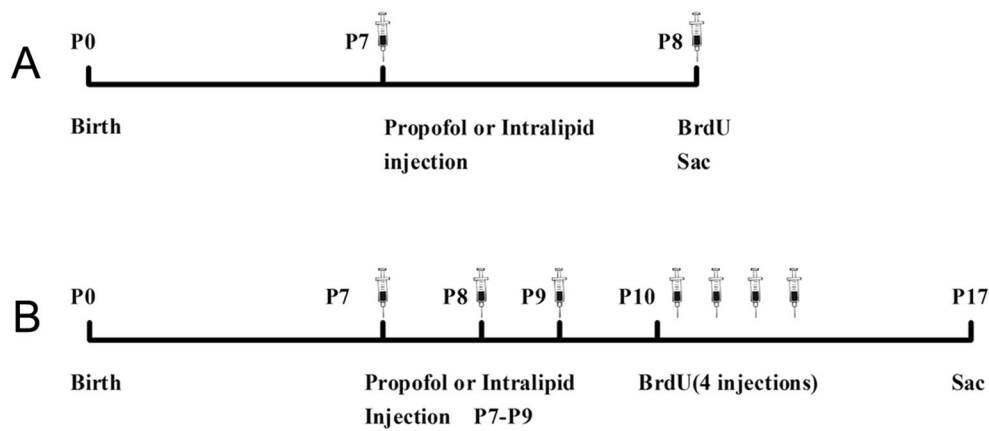
Fig. 1 Schematic diagram of the experimental procedures. **a** Mice were injected with propofol or intralipid at P7 and then injected with BrdU (50 mg/kg) at P8, animals were sacrificed 2 h after BrdU injection, and brains removed for immunohistochemistry or western blot. **b** Mice were injected with propofol or intralipid at P7–9 and then injected with BrdU (50 mg/Kg) at P10; animals were sacrificed at P17, and brains removed for immunofluorescence or Golgi staining

2 h, 37 °C) (Dako, Glostrup, Denmark), followed by the avidin-biotin complex (Dako, Glostrup, Denmark), and finally staining was visualized using the 3,3′-diaminobenzidine substrate kit (Vector Laboratories, Burlingame, CA, USA). For immunofluorescence, the sections were incubated with 488-conjugated anti-mouse IgG (at 1:500, 3 h; Jackson ImmunoResearch, West Grove, PA, USA). The sections were then mounted in Vectashield (Vector Laboratories) and counterstained with 4′,6-diamidino-2-phenylindole (DAPI) (Sigma-Aldrich, St. Louis, MO, USA) before being viewed and photographed using the Leica TCS SP2 spectral confocal laser-scanning microscope (Wetzlar, Germany).

BrdU immunohistochemistry was performed in cryostat sections according to the methods of Li et al. [28]. In brief, sections were incubated in 2 M HCl for 30 min at room temperature. This procedure was followed by neutralization in 0.05 M borate buffer (pH 8.5) for 15 min and blocking of endogenous peroxidase with 1 % H_2O_2 for 30 min. The sections were then immunostained with an anti-BrdU antibody (1:100, BD) overnight at 4 °C followed by biotinylated goat anti-mouse secondary antibody (1:200, Dako, Glostrup, Denmark) and avidin-biotin peroxidase complex (1:200, Dako, Glostrup, Denmark) for 2 h at room temperature. After the sections were washed in PBS, BrdU immunostaining was revealed by using 3,3-diaminobenzidine peroxidase (Vector Laboratories, Burlingame, CA, USA). For colocalization of BrdU and DCX, the sections were incubated with a mixture of primary antibodies including anti-BrdU (1:500, BD) and anti-DCX (1:100, Santa Cruz) at room temperature overnight, and a mixture of secondary fluorescence-tagged antibodies, Cy3 conjugated anti-rabbit (1:500, Jackson) and Alexa Fluor 488 conjugated (1:300, Invitrogen) at room temperature for 2 h. Rinsed sections were mounted onto gelatin-subbed slides and coverslipped with Vectashield (Santa Cruz). Images were

captured using a Zeiss Axiovert microscope equipped with a Zeiss AxioCam digital color camera (Oberkochen, Germany).

Western Blotting

The hippocampi were isolated and homogenized in ice-cold RIPA Lysis buffer (Beyotime, Shanghai, China). After centrifugation of lysates (15,000 g, 5 min at 4 °C), the protein concentration was determined via the Bicinchoninic Acid Kit (Beyotime Institute of Biotechnology, Shanghai, China). Protein samples (50 μg per lane) were separated on a 12 % SDS-polyacrylamide gel for 40 min at 120 V and then transferred onto a nitrocellulose (NC) membrane for 70 min at 120 V. The membranes were blocked with Tris-buffered saline (TBS), containing 0.1 % Tween 20 (TBST) and 5 % fat-free milk for 1 h at RT. The membranes were then incubated (overnight, at 4 °C) with the rabbit antibodies against Sox2 (1:1000, Chemicon), p-ERK1/2 or total-ERK1/2 (1:1000, Cell signaling), p-Akt or total-Akt (1:1000, Cell signaling), β-actin and GAPDH (1:2000, Cell Cwbio, Beijing, China), followed by 1 h of RT incubation with a peroxidase-conjugated goat anti-rabbit immunoglobulin G (IgG, 1:2000; Santa Cruz Biotechnology). Final visualization was achieved using an enhanced chemiluminescence Western blotting analysis system (Pierce, Rockford, IL, USA), and the signals were exposed to X-ray films (Kodak, Rochester, NY, USA) and analyzed with a Gel-Pro analyzer (Quantity One 4.0; Bio-Rad Laboratories). Western blots were obtained from the hippocampi of three animals of each group at P8. Quantification of total protein was determined relative to GAPDH, whereas phospho-protein was determined relative to total protein for the same experiments. Ratios of total protein/GAPDH or phospho-protein/total protein were obtained for each experiment and averaged.

Data are displayed as a percentage of normalized values from controls with vehicle treatment.

Golgi Staining

We used the FD Rapid Golgi Stain kit (FD NeuroTechnologies) to perform Golgi staining following the manufacturer's protocol [29, 30]. Briefly, the freshly dissected brains from P17 followed by repeated injections from P7 to P9 were immersed in impregnation solution (made by mixing equal volumes of solutions A and B) and stored at room temperature for 2 weeks in the dark. The brains were then transferred into solution C and kept for 48 h at 4 °C in the dark. Afterward, they were sliced using a horizon sliding slicer (SM2010R; Leica, Nussloch, Germany) to a thickness of 100 μm and stained using standard staining procedures. Granule neurons in the identical area of the hippocampal SGZ of each group were selected randomly, and one to two equivalent-length dendritic segments from each neuron were chosen for quantification. The density and morphology of dendrite spines were manually quantified according to the criteria described.

C17.2 Neural Stem Cell Culture

According to previous methods, the mouse NSC line C17.2 was cultured in standard DMEM/F12 (Invitrogen) supplemented with bovine serum (FBS, Gibco, USA) and 100 U/ml penicillin and streptomycin (Gibco, USA) at 37 °C in a humidified atmosphere containing 5 % CO_2 [31, 32].

The cell density of C17.2 in our experiment was about 4×10^4/ml, and each coverslip was planted about 2×10^4 cells. The cells for each FACS analysis were about 5×10^4 (counting the cell loss during the procedure). Every experiment, proliferation, FACS analysis, or apoptosis assay was set up four dose groups (DMSO, 10, 50, and 100 μM) and three time point groups (6, 24, and 48 h). All the experiments were repeated three times, and all the cells used were about 3.24×10^6.

Cell Proliferation and Apoptosis Assay of C17.2

The cell proliferation assay of C17.2 was performed 6, 24, and 48 h after the cells were exposed to different doses of protocol according to our previous methods [33]. In brief, C17.2 cells were cultured on coverslips and then were fixed with 4 % paraformaldehyde for 15 min at room temperature. After permeabilized with 0.1 % Triton X-100 for 10 min and blocked nonspecific staining with 3 % BSA (Sigma-Aldrich) for 1 h at room temperature, the cells were then incubated with rabbit anti-Ki67 antibody (1:300, Abcam, UK) overnight at 4 °C. After being washed three times with PBS, the cells were incubated with secondary antibodies (Alexa Fluor® 568 goat anti-rabbit IgG, 1:500; Life Technologies, USA) for 1 h at 37 °C. Nuclei were stained with 4′,6-diamidino-2-phenylindole (DAPI, Beyotime, China).

The apoptosis of C17.2 exposed with protocol was analyzed with In Situ Cell Death Detection Kit (Roche, Indianapolis, IN, USA) according to the manufacturer' instructions. In brief, cells were fixed, permeabilized, and incubated with the mixture of enzyme solution (TdT) and Label Solution (fluorescein-dUTP; 1:9) for 1 h at 37 °C; after being washed three times with PBS, the nuclei of the cells were stained with DAPI (Beyotime, China).

After immunostaining, the cells were observed and analyzed using a fluorescence microscopy system (Leica, Germany). At least ten fields were counted for each slide. The number of cells in each field was measured by counting DAPI-positive nuclei. The ratio of Ki67 positive or terminal deoxy nucleotidyl transferase-mediated nick end labeling (TUNEL) stained cells was determined by calculating positive cells to the total number of cells. All operations were performed at least for three times.

FACS Analysis of the Cell Cycle of C17.2 Cells

The C17.2 cells were dissociated by trypsin-EDTA (Gibco), centrifuged, and washed with PBS twice. The cells were harvested 6, 24, and 48 h after propofol exposure according to our previous protocol. The cells were fixed in 70 % ethanol for at least 12 h at 4 °C. Then, the cells were stained by the CycletestTM Plus DNA Reagent Kit (BD). The results were detected by a FACSCalibur flow cytometer and analyzed by the ModFit 2.0 software (BD). For each sample, at least 20, 000 cells were analyzed and all the analyses were performed in three independent experiments.

Quantification

According to our previous methods [28, 34], quantification of BrdU- and Sox2-positive cells was based on regional analysis of the DG (GCL plus SGZ and hilus) at P8 from five animals for each group. Two sets of consecutive brain slices (40-μm thickness) selected from every fifth were collected from each animal at the same level of the hippocampus, starting at 2.8 mm posterior to the bregma. Each set of two consecutive slices totaling to five sections were stained for BrdU or Sox2.

The BrdU and BrdU/DCX double-labeled cells were quantified on a series of five selected coronal brain sections along the DG (Bregma −1.56 to −2.20 mm) at P17 using confocal images. A mean cell count per section was obtained from five animals for each group, and comparisons were made between groups. Only cells within the SGZ and the GCL of the DG

were included; cells without direct contact to the DG (located within the hilus) were excluded from counting.

Typically, stereological cell counting was performed for quantification of the total number of NeuN-stained neurons in the GCL. Serial 20-μm sections through the rostrocaudal extent of the DG were selected at 12-section intervals for immunofluorescent staining with the NeuN and counterstaining with DAPI to mark nuclei in the DG at P17. The total sum of the NeuN-positive cells traced was multiplied by positive cells in the GCL (plus SGZ) per section and series number to give the total number of NeuN-positive cells in the GCL. To obtain volume estimations of the granular zone, the Cavalieri principle was applied: a surface estimation (in mm^2) of the GCL at each level was obtained by boundary contour tracings using Stereo Investigator software (MicroBrightField, Williston, VT, USA). These were multiplied by 12 and then multiplied by the thickness of the sections (0.02 mm). Five animals per group were used for analysis.

Statistical Analysis

Data were analyzed using one-way analysis of variance followed by Fisher's protected least-significant difference post hoc test or a least significant difference multiple-comparison t test. A value of $p<0.05$ was considered to

be significant. Statistical analysis was performed using the Statistical Product and Service Solutions software V13.0 (SPSS, Chicago, IL, USA).
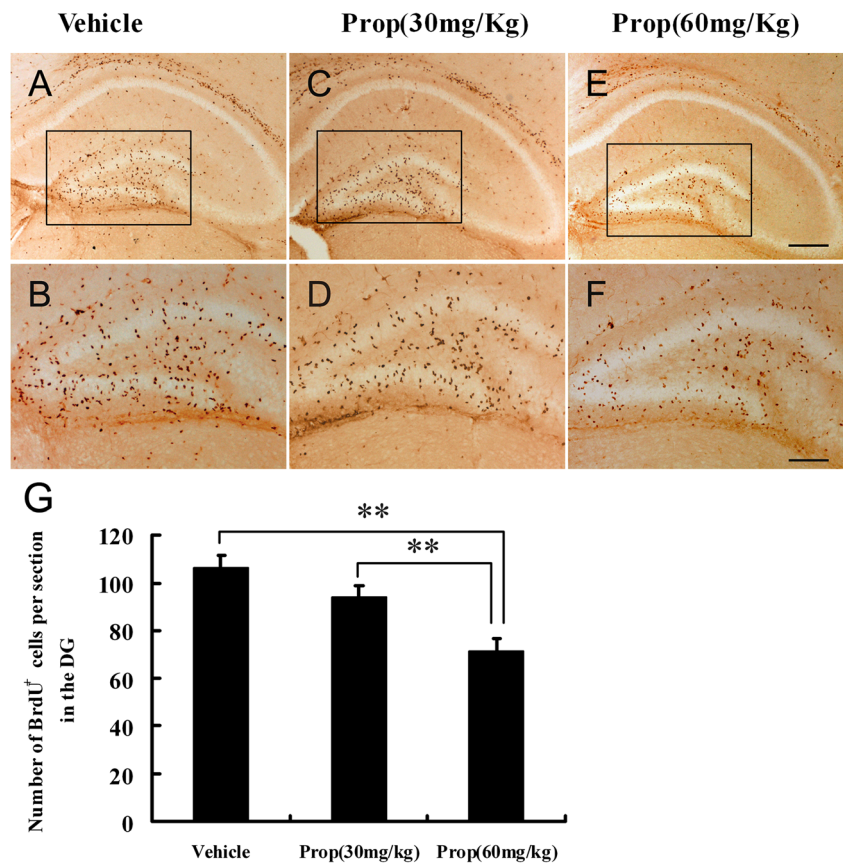
Results

1. Propofol inhibited BrdU-labeled progenitor proliferation in the DG of newborn mice in a dose-dependent manner.

   Two hours after BrdU administration, intense BrdU labeling of proliferating cells was observed in the DG of the 8-day-old mice. The most intense BrdU-labeled cells were found in the GCL and hilus, and scattered cells were also observed in the molecular layer (Fig. 2a–f). Newly born cells were irregularly shaped and often appeared in clusters. There was no difference in BrdU-positive cells in the DG between pups treated with 30 mg/kg propofol and pups treated with vehicle (105 ± 5, vehicle and 94 ± 4, prop 30 mg/kg, $n=5$, $p>0.05$). However, pups treated with 60 mg/kg propofol had decreased BrdU-positive cells in the DG compared to pups treated with vehicle (105 ± 5, vehicle and 71 ± 5, prop 60 mg/kg, $n=5$, $p<0.01$) (Fig. 2g).

2. Propofol decreased the Sox2-labeled NPCs in the DG of newborn mice in a dose-dependent manner.

Fig. 2 Propofol treatment decreased BrdU-labeled nuclei in the DG. **a–f** Representative images of BrdU-immunolabeled coronal sections of the DG of vehicle (**a**, **b**), propofol (30 mg/kg) (**c**, **d**), and propofol (60 mg/kg) (**e**, **f**) groups. Proliferating cells in the DG, labeled with BrdU at P8, 24 h postinjection of propofol (30 mg/kg), were not altered significantly compared with vehicle-injected animals. However, propofol (60 mg/kg) treatment decreased BrdU-positive cells in the DG significantly compared with vehicle treatment. *Scale bar*: **e**=200 μm for **a**, **c**, and **e**; **f**=100 μm for **b**, **d**, and **f**. **g** Quantitative analysis of the number of BrdU-labeled cells in the hippocampal DG. Data are presented as the mean cells in DG per section± SEM. $n=5$ mice per group. **$p<0.01$
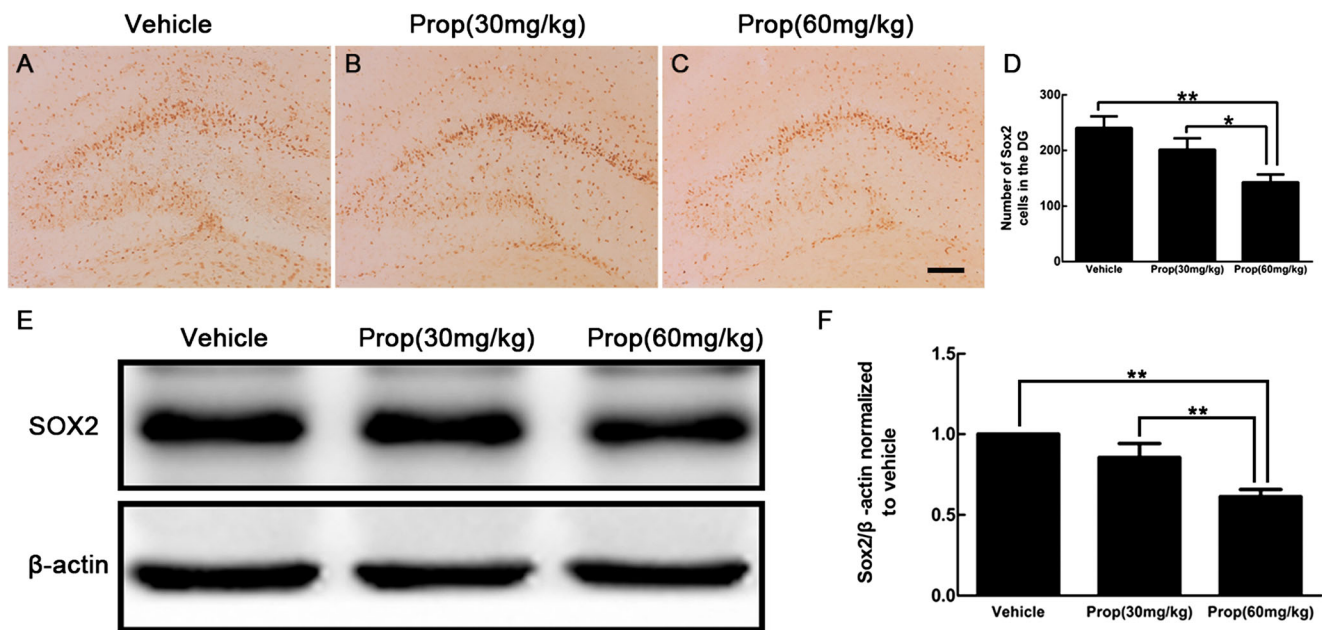
Fig. 3 Propofol treatment decreased Sox2 expression in the hippocampus. **a–f** Representative images of Sox2-immunolabeled coronal sections of the DG of vehicle (**a**), propofol (30 mg/kg) (**b**), and propofol (60 mg/kg) (**c**) groups. *Scale bar*: **c**=100 μm for **a–c**. **d** Quantitative analysis of the number of Sox2-labeled cells in the hippocampal DG. Data are presented as the mean cells in the DG per section±SEM. *n*=5 mice per group. *$p<0.05$, **$p<0.01$. **e** Western blots revealed reductions in Sox2 expression in the propofol (60 mg/kg)-treated mice compared with vehicle or propofol (30 mg/kg) groups. **f** The graph presents changes in the expressions of Sox2 in the hippocampal lysates indicating a reduction induced by propofol (60 mg/kg) treatment. Results are presented as means±SEM (*n*=3 mice/group). **$p<0.01$

To assess whether propofol affected the number of NPCs in the DG of newborn mice, we compared the number of Sox2-labeled NPCs among the three groups. As indicated in Fig. 3, there were no significant changes in the number of Sox2-positive cells in the DG of the propofol administration 30 mg/kg group (Fig. 3b, d) compared with the vehicle treatment group (Fig. 3a, d), whereas propofol administration at a dosage of 60 mg/kg decreased the number of Sox2-positive cells in the DG (Fig. 3c, d) as compared with that in the vehicle treatment group (Fig. 3a, d). Western blots revealed that Sox2 protein levels were lower in the hippocampi lysates from mice treated with 60 mg/kg propofol compared with vehicle treatment (Fig. 3e, f). These data suggest that the
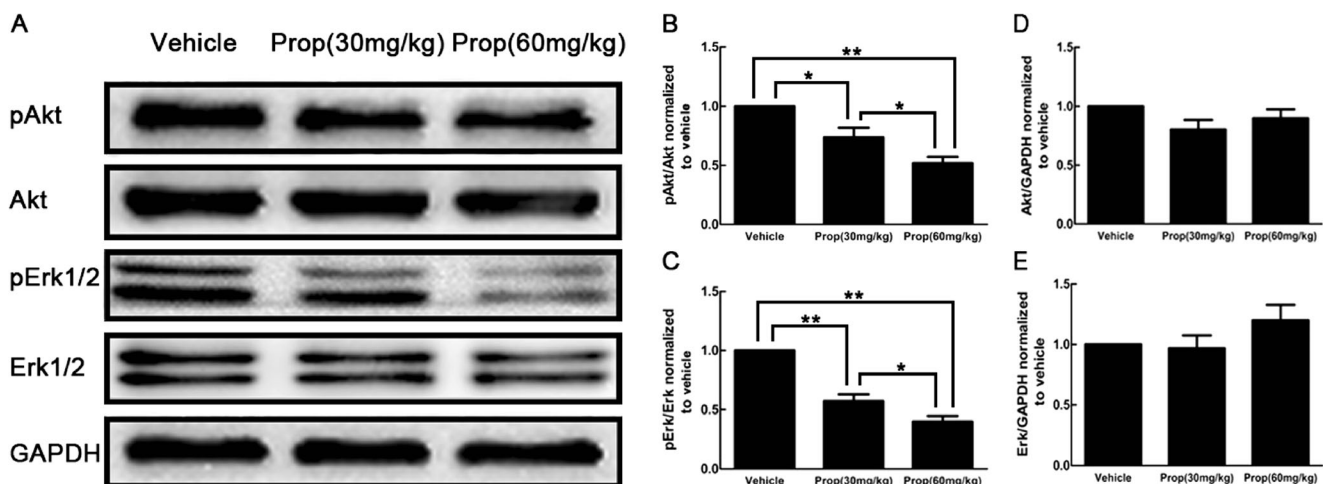

Fig. 4 Propofol inhibited ERK or Akt signaling in the hippocampus at P8. **a** Representative Western blots of hippocampal lysates from mice treated with vehicle or propofol (30 or 60 mg/kg). The levels of propofol-induced pAkt (**b**) and pERK1/2 (**c**) activation, expressed as a fold increase above baseline of vehicle-treated controls, were determined by densitometric analysis of the ratio pAkt/Akt or pERK1/2/ERK1/2. The levels of propofol induced total Akt (**d**) or ERK1/2 (**e**), expressed as a fold increase above baseline of vehicle-treated controls, were determined by densitometric analysis of the ratio Akt/GAPDH or ERK1/2/GAPDH. Results are presented as means±SEM (*n*=3 mice/group). *$p<0.05$, **$p<0.01$

high dose of propofol administration in the newborn mice at P7 directly induced a reduction of the number of NPCs in the DG.

3. Propofol reduced the activation of MAPK and Akt in the hippocampus of newborn mice.

ERK/mitogen-activated protein kinase (MAPK) and PI3K/Akt signaling pathways have been indicated to play important roles in the regulation of cell proliferation [26]. In the present study, impaired NPC proliferation was observed in the DG of mice injected with propofol. It was therefore of interest to examine the effect of propofol on ERK and Akt regulation in the hippocampus. The levels of pERK and pAkt were considerably lower in the hippocampi of newborn mice following propofol treatment at a dose of 30 mg/kg, and further reduction was induced at a dose of 60 mg/kg (Fig. 4a). The statistical analysis revealed that the propofol treatment (30 or 60 mg/kg) decreased the pAkt expression level (Fig. 4b) by 26 or 49 % compared with that of the vehicle-treated group, respectively, and propofol treatment (30 or 60 mg/kg) decreased the pERK immunoreactivity by 43 or 61 % compared with those of the vehicle-
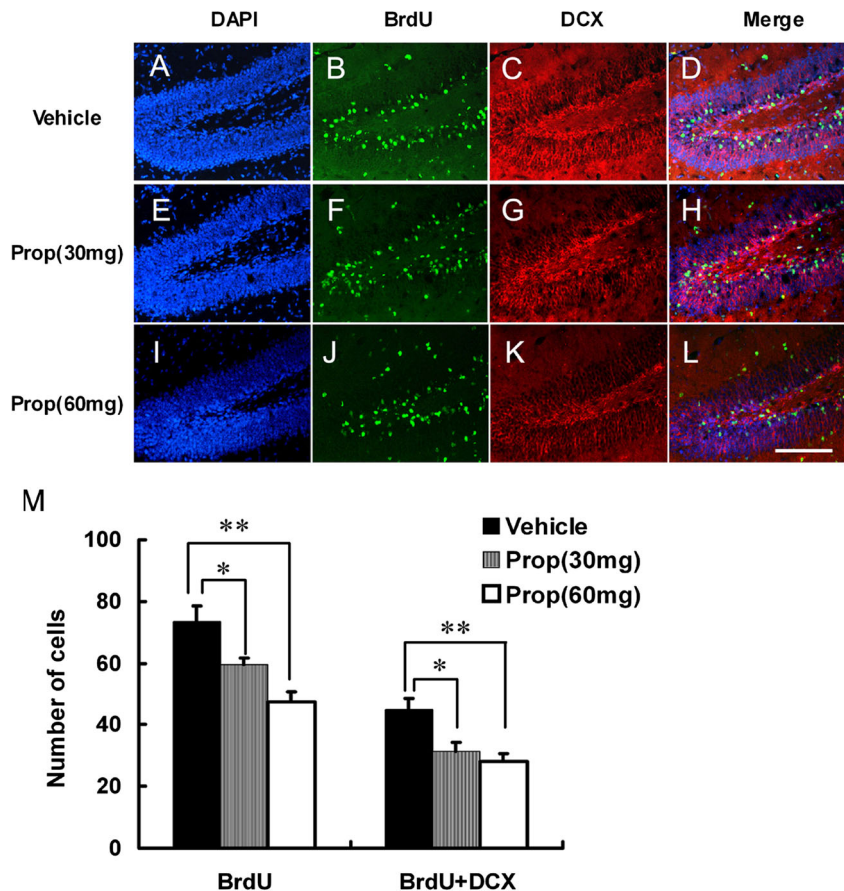
treated control group (Fig. 4c). These reductions induced by propofol treatment are mainly due to a decrease in phosphorylation, because the total levels of both ERK and Akt were not altered (Fig. 4d, e).

4. Propofol inhibited neurogenesis within the DG of newborn mice.

To assess the impact of propofol on early postnatal neurogenesis, we performed double staining with BrdU and DCX (markers for migrating neuroblasts or newly formed neurons) on P17. Each cell was assessed for its staining with antibodies against DCX and BrdU and the colocalization of these markers (Fig. 5). The results revealed that propofol treatment both at 30 and 60 mg/kg decreased the number of BrdU-positive cells and DCX/BrdU double-labeled cells in the GCL of the newborn mice as compared with the control group. These findings suggest that propofol suppresses neurogenesis within the hippocampus when administered to infant mice between P7 and P9.

NeuN is a neuron-specific nuclear protein that marks mature neurons [35]. The expression level of NeuN was assayed to examine the effect of early propofol treatment on neuronal maturation in the DG of mice on P17

Fig. 5 Propofol treatment suppress neurogenesis in the DG. **a**–**l** Immunolabeling for BrdU (*green*), DCX (*red*), DAPI (*blue*), and their merged images in the mouse DG of the vehicle group (**a**–**d**), propofol (30 mg/kg)-treated group (**e**–**h**), and propofol (60 mg/kg)-treated group (**i**–**l**). Note that propofol treatment decreased BrdU-positive cells and DCX/BrdU double-labeled cells. *Scale bar*: **l**=50 μm for **a**–**l**. **m** Quantification of BrdU-positive cells and DCX/BrdU double-labeled cells. Data are presented as the mean cells in the granular cellular layer per section±SEM. *n* =5 mice per group. *$p<0.05$, **$p<0.01$

(Fig. 6a–f). With DAPI staining, we found that gross anatomical structures were similar among three groups, and no significant alteration in the volume of GCL (Fig. 6g). There was no difference in the total number of NeuN-positive cells in the GCL between pups treated with 30 mg/kg propofol and pups treated with vehicle. However, pups treated with 60 mg/kg propofol had decreased NeuN-positive cells in the GCL compared to pups treated with vehicle ($p < 0.05$) (Fig. 6h).

5. Propofol reduced spine density and mushroom-type spines of granule cells in the DG of infant mice.

 To investigate the dendritic morphology of granule neurons of the DG following propofol treatment in P17 mice, we performed Golgi staining. The results revealed that the density of the dendritic spines was significantly reduced in the spared granular neurons in the propofol treatment (30 or 60 mg/Kg) group from 24 ± 2.0 to 17 ± 1.3 or 13 ± 1.4 per 20 μm of length of dendrite (Fig. 7a, b) ($p < 0.01$). This decrease was accompanied by a lower proportion of mushroom-type spines (vehicle 50.6 ± 2.6 %; prop 30 or 60 mg/kg 35.3 ± 3.1 % or 36.8 ± 2.2 %, $p < 0.001$) and a concomitant increase of thin spines (vehicle 18.3 ± 2.6 %; prop 30 or 60 mg/kg 31.9 ± 3.4 % or 30.2 ± 3.5 %, $p < 0.01$) (Fig 7c). There were no significant differences in the stubby-shaped spines among the three groups.

6. Propofol influenced cell proliferation of NSCs in a dose-dependent manner.

To assess the impact of propofol on cell proliferation of NSCs, we performed with Ki67 staining of C17.2 cell line. It demonstrated that 50 and 100 μM propofol exposure for 6, 24, and 48 h decreased the ratio of Ki67-positive cells significantly compared with the DMSO-treated control group (Fig. 8a–d). Propofol at the dosage of 10 μM showed no significant effect on the percentage of Ki67-positive cells when exposed for 6 and 24 h, while it markedly decreased the ratio of Ki67-positive cells when treated for 48 h (Fig. 8a–d).

The mitosis for all propofol concentrations and control rose from 6 h, got highest after 24 h, and then decreased on 48 h. The mitotic ratio of cells treated with 100 μM propofol decreased from 6 to 48 h of the experiment. Fifty micromolar propofol inhibited the cell mitosis 6 and 48 h compared with the control group. The mitosis ratio of cells treated with 10 μM propofol showed no significance compared with control after exposed for 6 and 24 h, while it inhibited cell mitosis after exposed for 48 h (Fig. 9a–o). The results of the cell cycle analysis support the conclusion that propofol inhibited the proliferation of C17.2 cells, which is consistent with analysis of cell proliferation using Ki67 staining.

7. Propofol exposure influenced the apoptosis of C17.2 NSCs in a dose-dependent manner.

 Apoptosis was increased as the concentration of propofol increased over the clinically relevant concentration (10 μM). The ratio of TUNEL-positive cells was significantly increased when C17.2 NSCs were

Fig. 6 Propofol treatment decreased NeuN expression in the DG at P17. **a–c** Example images of DG sections immuno-stained with NeuN and counterstained with DAPI. A higher magnification of NeuN-labeled cells in the suprapyramidal blade of the DG of each group is shown in **d–f**. *Scale bars*: **c**=200 μm for **a–c**; **f**=20 μm for **d–f**. **g**, **h** Quantification of volume of the GCL (**g**) and total number of NeuN-positive cells in the GCL (**h**). Values represent mean± SEM. $n=5$ mice per group. $*p < 0.05$
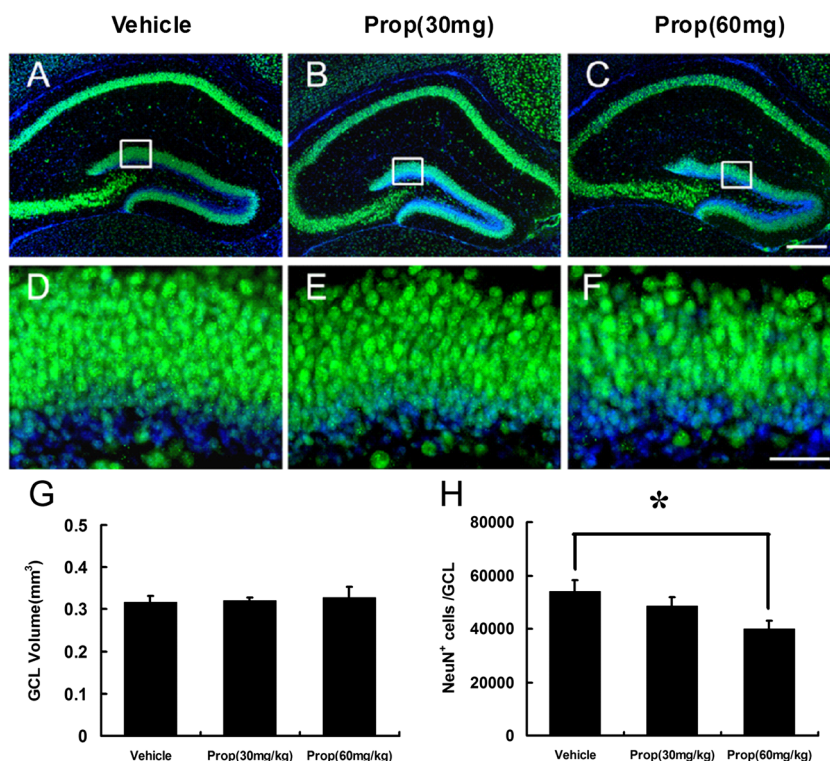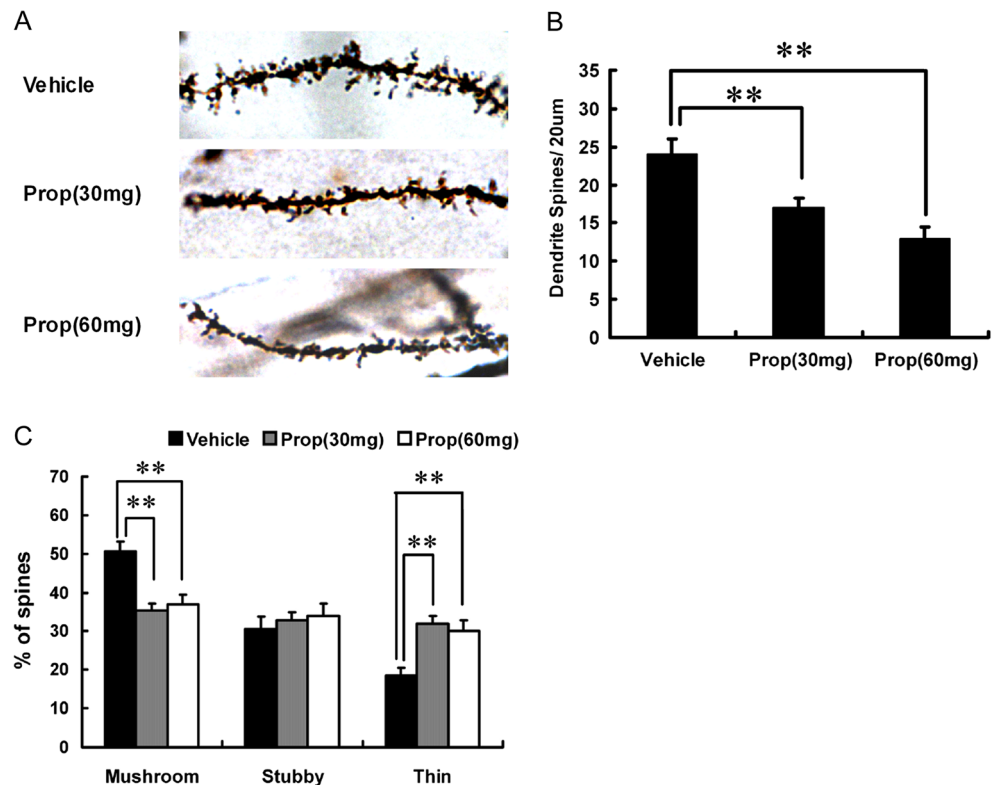
Fig. 7 Propofol treatment induces degeneration of dendritic spines of DG granule neurons. **a** Representative dendrites for DG granule neurons for vehicle and propofol treatment (30 or 60 mg/kg) groups. **b** Averaged spine density in the DG granule neurons was significantly reduced by propofol treatment. **c** Propofol-treated mice had more thin spines and mushroom-shaped spines than the vehicle-treated group. All values in **b** and **c** represent mean± SEM. $n=3$ mice per group. $**p<0.01$

exposed in 50 and 100 μM propofol for 24 and 48 h compared with the DMSO-treated group in a dose-dependent manner (Fig. 10a–d). Propofol at the dosage of 10 μM showed no significant effect on the ratio of TUNEL-positive cells even when treated for 48 h (Fig. 10a–d).

Discussion

In this study, we studied the effects of propofol at different doses on cell proliferation and neurogenesis in the DG of mice during the first two postnatal weeks. Our results indicate that a single injection of propofol at a dosage of 60 mg/kg markedly suppresses the cell proliferation and early neurogenesis in the infant mouse DG. Propofol at a dose of 30 mg/kg elicited a less pronounced suppression of the hippocampal early neurogenesis, with no significant influences on the cell proliferation in the DG of newborn mice. In vitro results demonstrated that propofol at a clinically relevant concentration (10 μM) produced no significant effect on the cell proliferation and apoptosis of NSCs when treated less than 48 h; however, higher dose of propofol markedly inhibited cell proliferation and activated apoptosis of NSCs.

Postnatal cell proliferation in the SGZ of the DG is age dependent and related to learning and memory [18, 36, 37]. We found that exposure to propofol significantly decreased the hippocampal cell proliferation as assessed by BrdU, in the DG at P8 in a dose-dependent manner. These results are seemingly contradictory to recent observations indicating that the general anesthetic propofol does not affect new cell proliferation in the DG of young or aged rats [21]. These findings might be due to the effect of propofol on the proliferation of hippocampal cells in the DG in an age-dependent manner, and the developing brain at this stage is more sensitive to propofol and vulnerable to anesthetic-induced damage [25].

Recent studies have reported that the transcription factor Sox2, a key regulator of neuronal stem cells, is highly expressed in the NPCs localized in the SGZ [38]. *SOX2* activates target genes, such as nestin and sonic hedgehog, to determine the maintenance of NPC properties including proliferation and self-renewal [39]. We confirmed that infant mice exposure to propofol significantly decreased both Sox2-positive cells in the DG and the Sox2 protein level in the hippocampi at P8 in a dose-dependent manner, which suggests NPCs are sensitive to propofol treatment. In addition, a recent study reported that Sox2 can prevent programmed cell death by activating expression of the survivin gene in neural stem cells [40]. This might explain why propofol at a dosage over
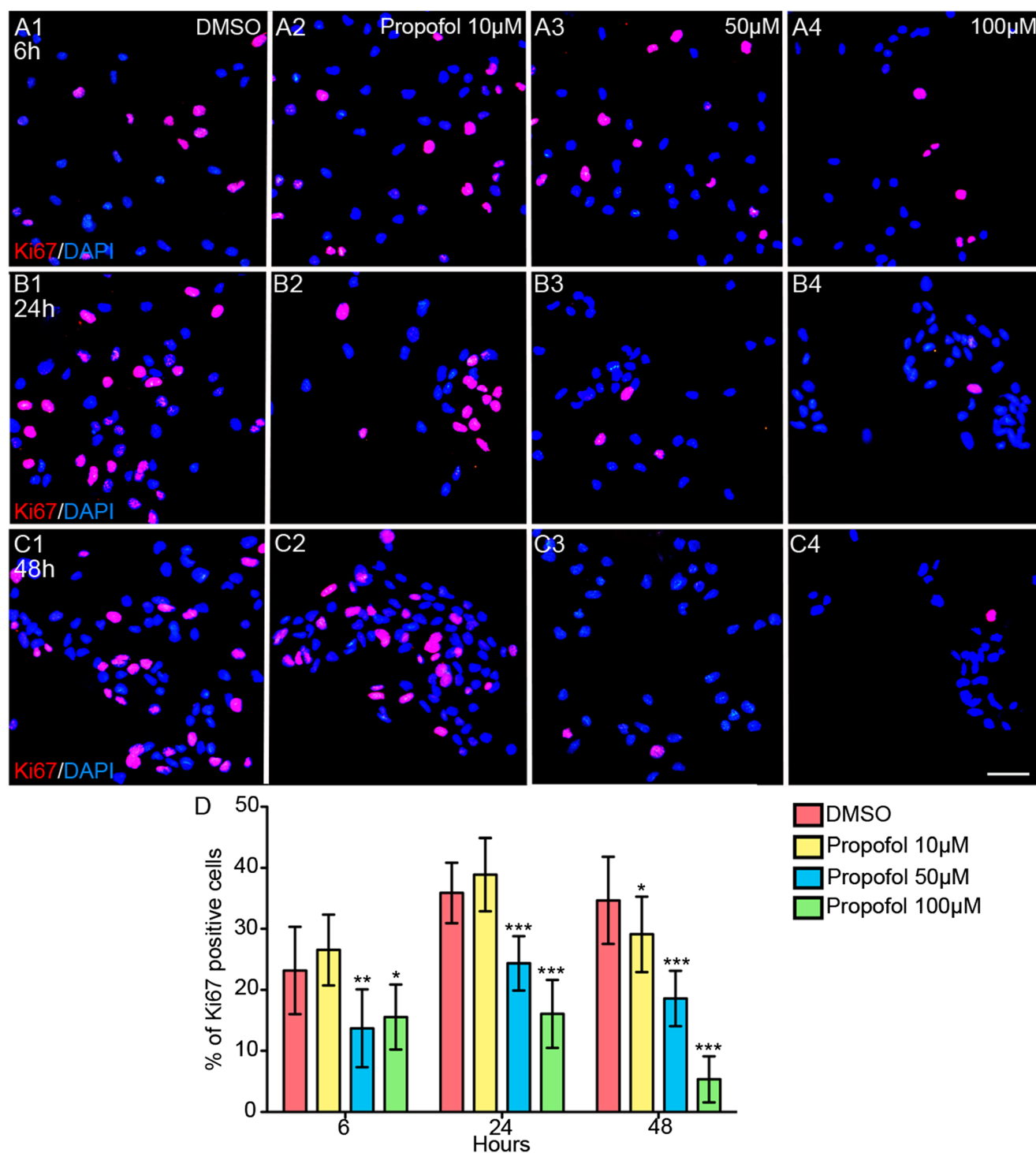
Fig. 8 Propofol treatment influenced the proliferation of C17.2 cells in a dose-dependent manner. **a–c** Representative images of C17.2 cells stained with Ki67 (*red*) and DAPI (*blue*) when exposed to propofol at different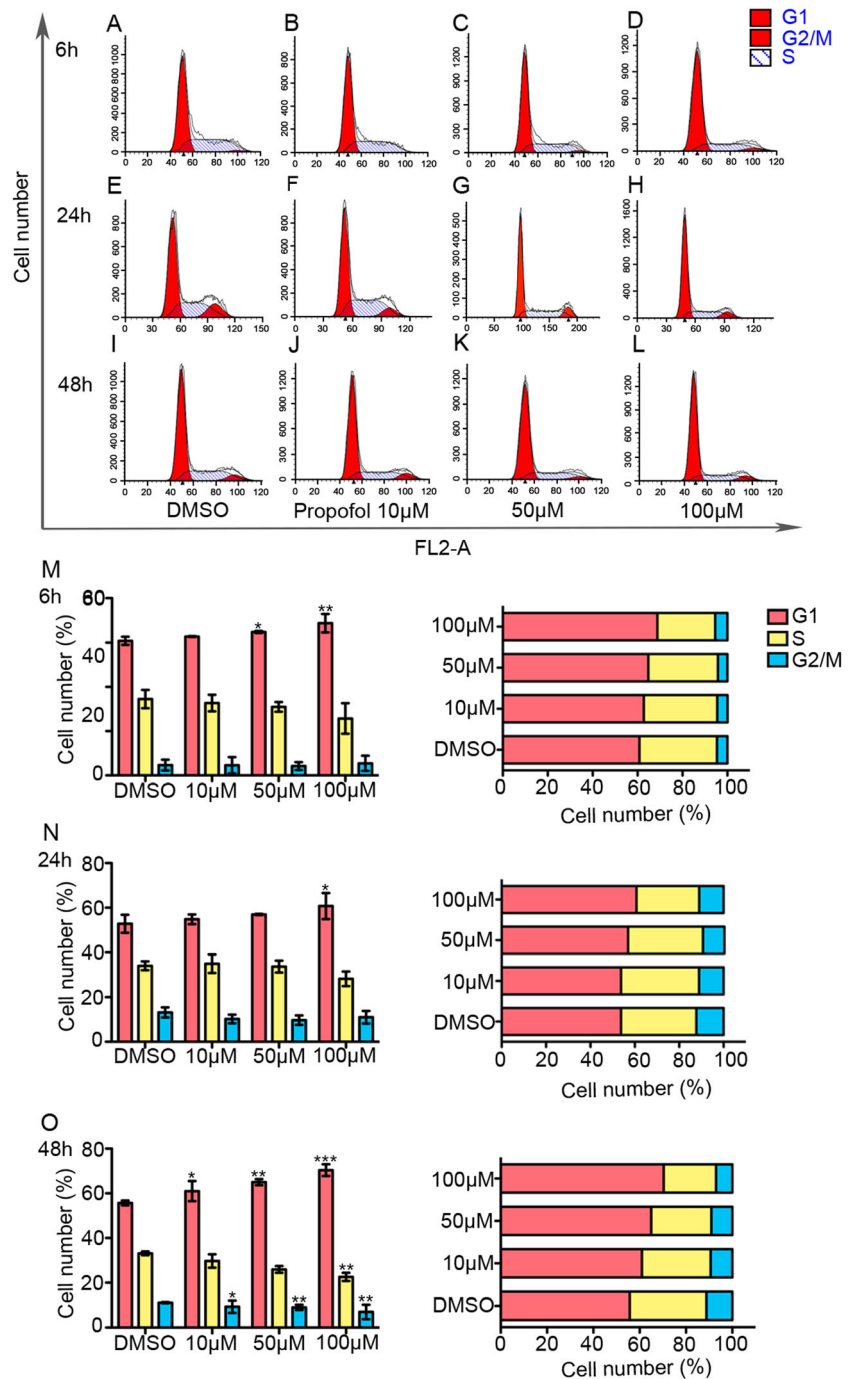 dosages (10, 50, and 100 μM) for 6, 24, and 48 h. *Scale bars*= 50 μm. **d** Statistical analysis of the ratio of Ki67-positive cells. Data from at least three independent experiments are expressed as the mean±SD. *$p<0.05$, **$p<0.01$, ***$p<0.001$, versus DMSO-treated cells

50 mg/kg typically causes a significant neuroapoptosis response in infant mice.

Multiple mechanisms may mediate antiproliferative action of propofol. Both the ERK and Akt signaling pathways act as effectors of neurotrophin signaling and might contribute to proliferation. One study has demonstrated that propofol administration (25 mg/kg) induced pERK1/2 and pAkt upregulation in the cortex and

Fig. 9 Cell cycle analysis of C17.2 cells exposed to propofol at different dosages for 6, 24, and 48 h. **a–l** Representative FACS analysis cell-cycle data of C17.2 cells exposed to propofol at different dosages (10, 50, and 100 μM) for 6, 24, and 48 h. **m–o** Statistical analysis. Data from three separate experiments are expressed as the mean±SD. *$p<0.05$, **$p<0.01$, ***$p<0.001$, versus DMSO treated cells

downregulation in the thalamus of P14 rats [26]. Our study indicated that both pERK and pAkt were inhibited by propofol treatment, indicating these two signaling pathways were involved in the proliferation of NPCs in the DG. Noticeably, propofol at a low dose resulted in decreased levels of pERK and pAkt, and we believe those two pathways are active early in the proliferation of NPCs. The discrepancy of the influence of propofol on pERK and pAkt in different brain regions might depend on neurotrophin levels or propofol dose.

Using double immunohistological labeling for BrdU and DCX, we were able to verify significant inhibition of postnatal neurogenesis within the DG by repeated injections from P7 to P9. Within the SGZ and the inner third of the GCL of the DG, we identified BrdU-positive cells and BrdU/DCX double-stained cells.
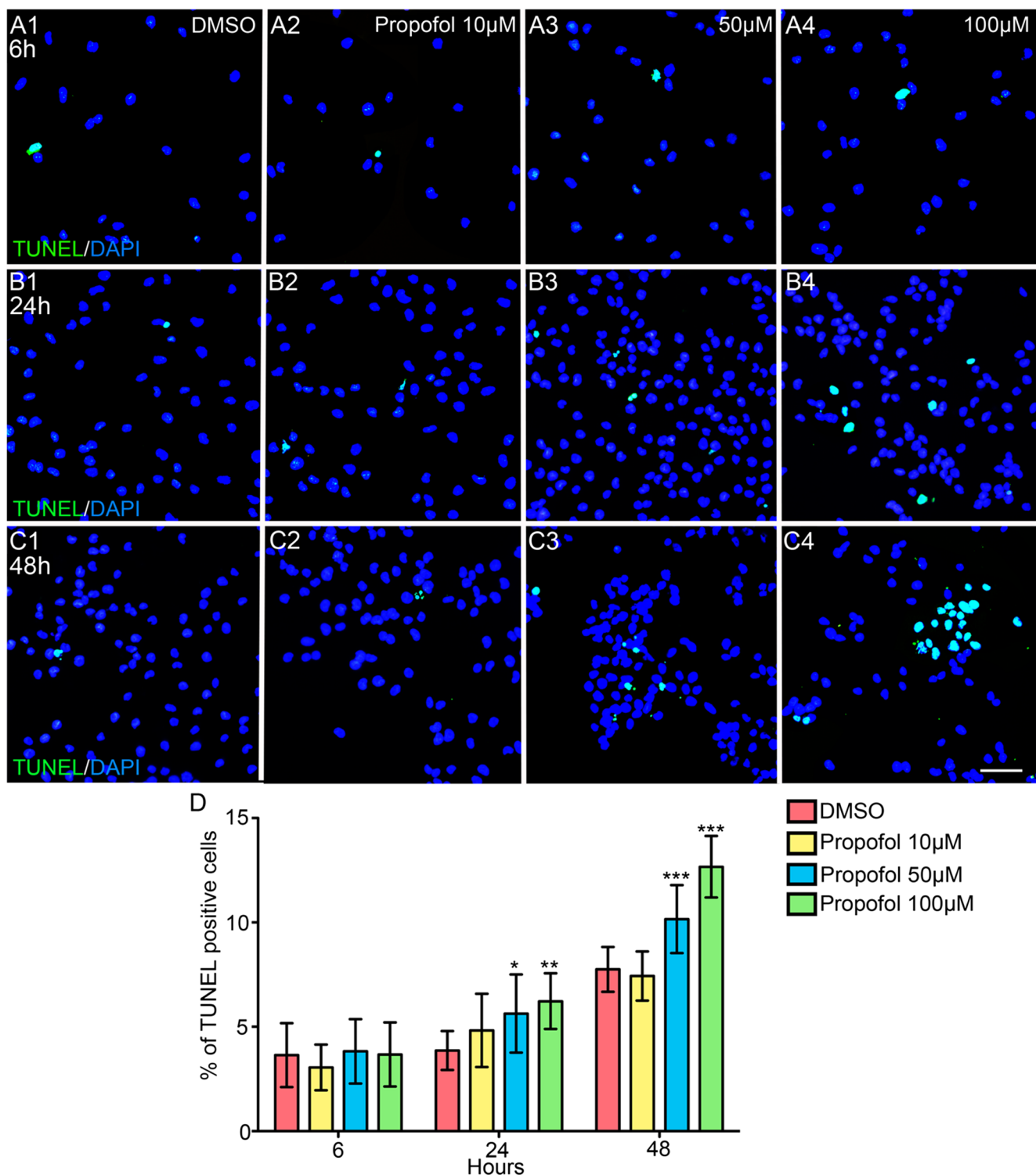
Fig. 10 Propofol treatment influenced the apoptosis of C17.2 cells in a dose-dependent manner. **a–c** Representative images of C17.2 cells stained with TUNEL (*green*) and DAPI (*blue*) when exposed to propofol at different dosages (10, 50, and 100 μM) for 6, 24, and 48 h.

Scale bars=50 μm. **d** Statistical analysis of the ratio of TUNEL-positive cells. Data from at least three independent experiments are expressed as the mean±SD. *$p<0.05$, **$p<0.01$, ***$p<0.001$, versus DMSO-treated cells

These double-labeled cells were immature neurons that were generated during the period of BrdU injection (at P7–P9) and had differentiated toward a neuronal phenotype that could be significantly inhibited by propofol treatment. One recent study indicated that propofol postconditioning exerted long-term protection

against cerebral ischemia partially by promoting neurogenesis in the DG in a rat focal ischemia model [41]. This seemly suggests propofol exerts different effects on DG neurogenesis depending on stress level.

In addition, NeuN-labeled mature neurons in the DG were also decreased by propofol treatment. This was further confirmed by analysis of the density and morphology of dendrite spines induced by propofol treatment. We demonstrated that propofol treatment impaired the maturation of neurons generated after anesthesia as indicated by lower density of dendrite spines. Similarly, one new finding confirmed that a significant reduction in the dendrite maturation induced by propofol treatment mainly occurred in the neurons generated by 17 days, and not 11 days, before anesthesia. These findings particularly infer that maturation of newborn neurons generated before or after anesthesia is extremely sensitive to propofol treatment. It is well known that the spine number and structural plasticity are tightly correlated with synaptic function in the mammalian brain, and thin spines are associated with immature synapses and mushroom spines are associated with mature and stable synapses [14, 42]. Mushroom spine decreases due to propofol treatment might be a possible mechanism to explain cognitive decline due to destruction of dendritic spine stability induced by propofol treatment.

In conclusion, propofol treatment significantly impaired cell proliferation and inhibited early neurogenesis in immature mouse brains. Our results demonstrated, for the first time, the potential negative effect of propofol exposure during early postnatal life. These findings need to be confirmed in future investigations, as the results might have a high relevance and impact on the clinical application of propofol, as the anesthetic is typically used during pediatric surgery on neonates and young children.

References

1. Istaphanous GK, Loepke AW (2009) General anesthetics and the developing brain. Curr Opin Anesthesiol 22(3):368–373
2. McCann ME, Soriano SG (2012) General anesthetics in pediatric anesthesia: influences on the developing brain. Curr Drug Targets 13 (7):944–951
3. Reddy SV (2012) Effect of general anesthetics on the developing brain. J Anaesthesiol Clin Pharmacol 28(1):6–10
4. Jevtovic-Todorovic V, Hartman RE, Izumi Y, Benshoff ND, Dikranian K, Zorumski CF, Olney JW, Wozniak DF (2003) Early exposure to common anesthetic agents causes widespread neurodegeneration in the developing rat brain and persistent learning deficits. J Neurosc: Off J Soc Neurosci 23(3):876–882
5. Cattano D, Young C, Straiko MM, Olney JW (2008) Subanesthetic doses of propofol induce neuroapoptosis in the infant mouse brain. Anesth Analg 106(6):1712–1714
6. Fredriksson A, Ponten E, Gordh T, Eriksson P (2007) Neonatal exposure to a combination of N-methyl-D-aspartate and gamma-aminobutyric acid type A receptor anesthetic agents potentiates apoptotic neurodegeneration and persistent behavioral deficits. Anesthesiology 107(3):427–436
7. Ikonomidou C (1999) Blockade of NMDA receptors and apoptotic neurodegeneration in the developing brain. Science 283(5398):70–74
8. Satomoto M, Satoh Y, Terui K, Miyao H, Takishima K, Ito M, Imaki J (2009) Neonatal exposure to sevoflurane induces abnormal social behaviors and deficits in fear conditioning in mice. Anesthesiology 110(3):628–637
9. Yu D, Jiang Y, Gao J, Liu B, Chen P (2013) Repeated exposure to propofol potentiates neuroapoptosis and long-term behavioral deficits in neonatal rats. Neurosci Lett 534:41–46
10. Wilder RT, Flick RP, Sprung J, Katusic SK, Barbaresi WJ, Mickelson C, Gleich SJ, Schroeder DR, Weaver AL, Warner DO (2009) Early exposure to anesthesia and learning disabilities in a population-based birth cohort. Anesthesiology 110(4):796–804
11. Franks NP, Lieb WR (1994) Molecular and cellular mechanisms of general anaesthesia. Nature 367(6464):607–614
12. Hudson AE, Hemmings HC Jr (2011) Are anaesthetics toxic to the brain? Br J Anaesth 107(1):30–37
13. Irifune M, Takarada T, Shimizu Y, Endo C, Katayama S, Dohi T, Kawahara M (2003) Propofol-induced anesthesia in mice is mediated by gamma-aminobutyric acid-A and excitatory amino acid receptors. Anesth Analg 97(2):424–429, table of contents
14. Harris KM, Jensen FE, Tsao B (1992) Three-dimensional structure of dendritic spines and synapses in rat hippocampus (CA1) at postnatal day 15 and adult ages: implications for the maturation of synaptic physiology and long-term potentiation. J Neurosc: Off J Soc Neurosci 12(7):2685–2705
15. Stratmann G (2011) Review article: neurotoxicity of anesthetic drugs in the developing brain. Anesth Analg 113(5):1170–1179
16. Vutskits L (2012) Anesthetic-related neurotoxicity and the developing brain: shall we change practice? Paediatric Drugs 14(1):13–21
17. Ming GL, Song H (2005) Adult neurogenesis in the mammalian central nervous system. Annu Rev Neurosci 28:223–250
18. Deng W, Aimone JB, Gage FH (2010) New neurons and new memories: how does adult hippocampal neurogenesis affect learning and memory? Nat Rev Neurosci 11(5):339–350
19. Eichenbaum H (2004) Hippocampus: cognitive processes and neural representations that underlie declarative memory. Neuron 44(1):109–120
20. Winocur G, Wojtowicz JM, Sekeres M, Snyder JS, Wang S (2006) Inhibition of neurogenesis interferes with hippocampus-dependent memory function. Hippocampus 16(3):296–304
21. Erasso DM, Camporesi EM, Mangar D, Saporta S (2013) Effects of isoflurane or propofol on postnatal hippocampal neurogenesis in young and aged rats. Brain Res 1530:1–12
22. Erasso DM, Chaparro RE, del Rio CEQ, Karlnoski R, Camporesi EM, Saporta S (2012) Quantitative assessment of new cell proliferation in the dentate gyrus and learning after isoflurane or propofol anesthesia in young and aged rats. Brain Res 1441:38–46
23. Thal SC, Timaru-Kast R, Wilde F, Merk P, Johnson F, Frauenknecht K, Sebastiani A, Sommer C, Staib-Lasarzik I, Werner C (2014) Propofol impairs neurogenesis and neurological recovery and increases mortality rate in adult rats after traumatic brain injury. Crit Care Med 42(1):129–141
24. Krzisch M, Sultan S, Sandell J, Demeter K, Vutskits L, Toni N (2013) Propofol anesthesia impairs the maturation and survival of adult-born hippocampal neurons. Anesthesiology 118(3):602–610

25. Sall JW, Stratmann G, Leong J, Woodward E, Bickler PE (2012) Propofol at clinically relevant concentrations increases neuronal differentiation but is not toxic to hippocampal neural precursor cells in vitro. Anesthesiology 117(5):1080–1090

26. Popic J, Pesic V, Milanovic D, Todorovic S, Kanazir S, Jevtovic-Todorovic V, Ruzdijic S (2012) Propofol-induced changes in neurotrophic signaling in the developing nervous system in vivo. PLoS One 7(4):e34396

27. Whittington RA, Virag L, Marcouiller F, Papon MA, El Khoury NB, Julien C, Morin F, Emala CW, Planel E (2011) Propofol directly increases tau phosphorylation. PLoS One 6(1):e16648

28. Li DB, Tang J, Xu HW, Fan XT, Bai Y, Yang L (2008) Decreased hippocampal cell proliferation correlates with increased expression of BMP4 in the APPswe/PS1DeltaE9 mouse model of Alzheimer's disease. Hippocampus 18(7): 692–698

29. Gao X, Deng P, Xu ZC, Chen J (2011) Moderate traumatic brain injury causes acute dendritic and synaptic degeneration in the hippocampal dentate gyrus. PLoS One 6(9):e24566

30. Yau SY, Lau BW, Tong JB, Wong R, Ching YP, Qiu G, Tang SW, Lee TM, So KF (2011) Hippocampal neurogenesis and dendritic plasticity support running-improved spatial learning and depression-like behaviour in stressed rats. PLoS One 6(9):e24263

31. Wang SJ, Weng CH, Xu HW, Zhao CJ, Yin ZQ (2014) Effect of optogenetic stimulus on the proliferation and cell cycle progression of neural stem cells. J membr Biol 247(6):493–500

32. Snyder EY, Deitcher DL, Walsh C, Arnold-Aldea S, Hartwieg EA, Cepko CL (1992) Multipotent neural cell lines can engraft and participate in development of mouse cerebellum. Cell 68(1):33–51

33. Chen X, Li QY, Xu HW, Yin ZQ (2014) Sodium iodate influences the apoptosis, proliferation and differentiation potential of radial glial cells in vitro. Cell Physiol Biochem 34(4):1109–1124

34. Fan XT, Xu HW, Cai WQ, Yang H, Liu S (2004) Antisense Noggin oligodeoxynucleotide administration decreases cell proliferation in the dentate gyrus of adult rats. Neurosci Lett 366(1):107–111

35. Mullen RJ, Buck CR, Smith AM (1992) NeuN, a neuronal specific nuclear protein in vertebrates. Development 116(1):201–211

36. Snyder JS, Hong NS, McDonald RJ, Wojtowicz JM (2005) A role for adult neurogenesis in spatial long-term memory. Neuroscience 130 (4):843–852

37. Kuhn HG, Dickinson-Anson H, Gage FH (1996) Neurogenesis in the dentate gyrus of the adult rat: age-related decrease of neuronal progenitor proliferation. J Neurosc: Off J Soc Neurosci 16(6):2027–2033

38. Pevny LH, Nicolis SK (2010) Sox2 roles in neural stem cells. Int J Biochem Cell Biol 42(3):421–424

39. Bonaguidi MA, Wheeler MA, Shapiro JS, Stadel RP, Sun GJ, Ming GL, Song H (2011) In vivo clonal analysis reveals self-renewing and multipotent adult neural stem cell characteristics. Cell 145(7):1142–1155

40. Feng R, Zhou S, Liu Y, Song D, Luan Z, Dai X, Li Y, Tang N, Wen J, Li L (2013) Sox2 protects neural stem cells from apoptosis via up-regulating survivin expression. Biochem J 450(3):459–468

41. Wang H, Luo M, Li C, Wang G (2011) Propofol post-conditioning induced long-term neuroprotection and reduced internalization of AMPAR GluR2 subunit in a rat model of focal cerebral ischemia/reperfusion. J Neurochem 119(1):210–219

42. Peters A, Kaiserman-Abramof IR (1970) The small pyramidal neuron of the rat cerebral cortex. The perikaryon, dendrites and spines. Am J Anat 127(4):321–355